NANO MICRO small

Supporting Information

for *Small*, DOI: 10.1002/smll.201604301

Direct Growth of High Mobility and Low-Noise Lateral MoS_2–Graphene Heterostructure Electronics

Amirhossein Behranginia, Poya Yasaei, Arnab K. Majee, Vinod K. Sangwan, Fei Long, Cameron J. Foss, Tara Foroozan, Shadi Fuladi, Mohammad Reza Hantehzadeh, Reza Shahbazian-Yassar, Mark C. Hersam, Zlatan Aksamija, and Amin Salehi-Khojin**

SUPPORTING INFORMATION

Direct Growth of High Mobility and Low Noise Lateral MoS_2-Graphene Heterostructure Electronics

Amirhossein Behranginia[1], Poya Yasaei[1], Arnab K. Majee[2], Vinod K. Sangwan[3], Fei Long[4], Cameron J. Foss[2], Tara Foroozan[5], Shadi Fuladi[6], Mohammad Reza Hantehzadeh[1], Reza Shahbazian-Yassar[1], Mark C. Hersam[3,7], Zlatan Aksamija[2], Amin Salehi-Khojin[1]**

[1]*Department of Mechanical and Industrial Engineering, University of Illinois at Chicago, Chicago, IL, 60607, USA*
[2]*Electrical and Computer Engineering Department, University of Massachusetts Amherst, Amherst, Massachusetts 01003, United States*
[3]*Department of Materials Science and Engineering, Northwestern University, Evanston, Illinois 60208, USA*
[4]*Department of Mechanical Engineering, University of Michigan Tech, Houghton, MI, 49931, USA*
[5]*Department of Civil and Material Engineering, University of Illinois at Chicago, Chicago, IL, 60607, USA*
[6]*Department of Physics, University of Illinois at Chicago, Chicago, IL, 60607, USA*
[7]*Department of Chemistry, Northwestern University, Evanston, Illinois 60208, USA*
[*] Corresponding author, salehikh@uic.edu, zlatana@engin.umass.edu

Table of contents:

S1. Polycrystalline MoS_2 film next to graphene flakes

By increasing the MoS_2 growth time, the polycrystalline MoS_2 film grows next to the graphene flakes and forms a lateral junction with them.

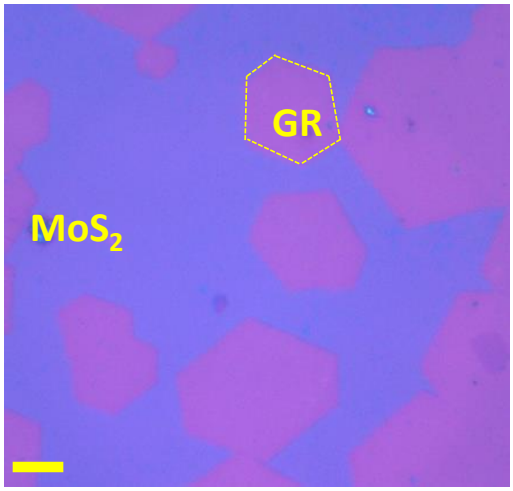

Figure S1. Optical image of the Polycrystalline MoS_2 film next to the graphene flakes (scale bar 10 µm).

S2. AFM characterization of the MoS_2/Gr interface

Due to the relatively large (25%) mismatch between the lattice parameters in graphene and MoS_2, we believe that covalent lateral bonding at an atomically sharp interface is not likely to happen without major crystalline distortion. Such a distortion is less significant in covalent lateral interfaces with higher lattice similarity such as MoS_2-WS_2 or graphene-hBN. As we discussed in the manuscript, the lateral MoS_2/Gr interfaces are formed due to the self-limiting growth process (deposition selectivity) which leads to a very narrow overlapping region. The paper by Ling *et al.*[1] has also shown that MoS_2/Gr interfaces exhibit a 2-30 nm wide overlapping region. However, no distortion is observed in the lattice parameters of graphene or MoS2 in the overlapping region, as evidenced by high-resolution transmission electron microscopy (HRTEM) images and their corresponding Fast Fourier transform (FFT) diffractograms.

To directly evaluate the overlapping region in our samples, we also performed atomic force microscopy on the MoS2-graphene interfaces. Figure S2 shows the SEM and AFM images of the interface. Particularly, Figure S2c shows that the overlapping region is narrower than 30 nm.

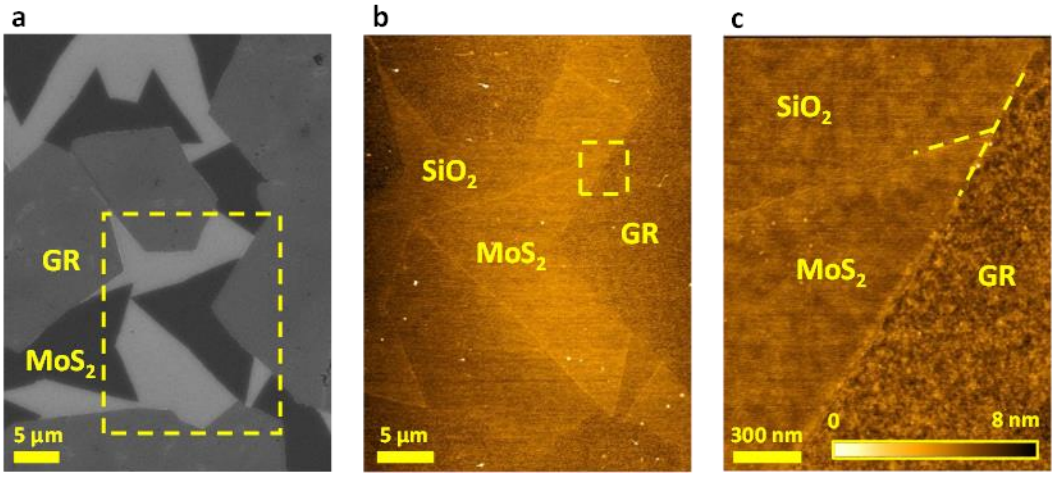

Figure S2. **(a)** SEM image of the MoS2-graphene in-plane heterostructure. **(b)** AFM image of the selected area of (a). **(c)** Higher magnification AFM image of the MoS2-graphene interface.

S3. Source-drain current-voltage characteristic of the MoS_2/Gr and MoS_2/Metal FETs

Two probe current-voltage (I_d-V_{ds}) measurements at a gate voltage of 60 V at different temperatures were carried out to investigate the output characteristics of the in-plane MoS_2/Gr (Fig. S3a) and MoS_2/Metal (Fig.S3b) field-effect transistor (FET).

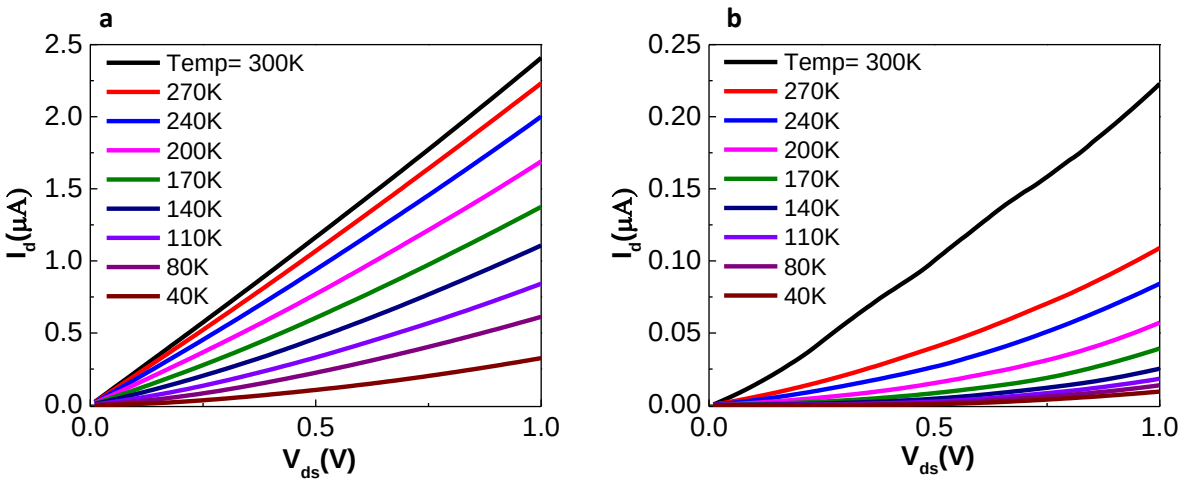

Figure S3. Output characteristic at different temperatures for **(a)** MoS_2/Gr **(b)** MoS_2/Metal FETs.

S4. Two-probe current-voltage measurements of the MoS_2/Gr and MoS_2/Metal FETs

The two-probe current-voltage measurements of the MoS_2/Gr and MoS_2/Metal FETs under different applied gate voltages at three different temperatures (300K, 240K and 200K) show an Ohmic behavior for MoS_2/Gr FET, while they show Schottky behavior for MoS_2/Metal FET.

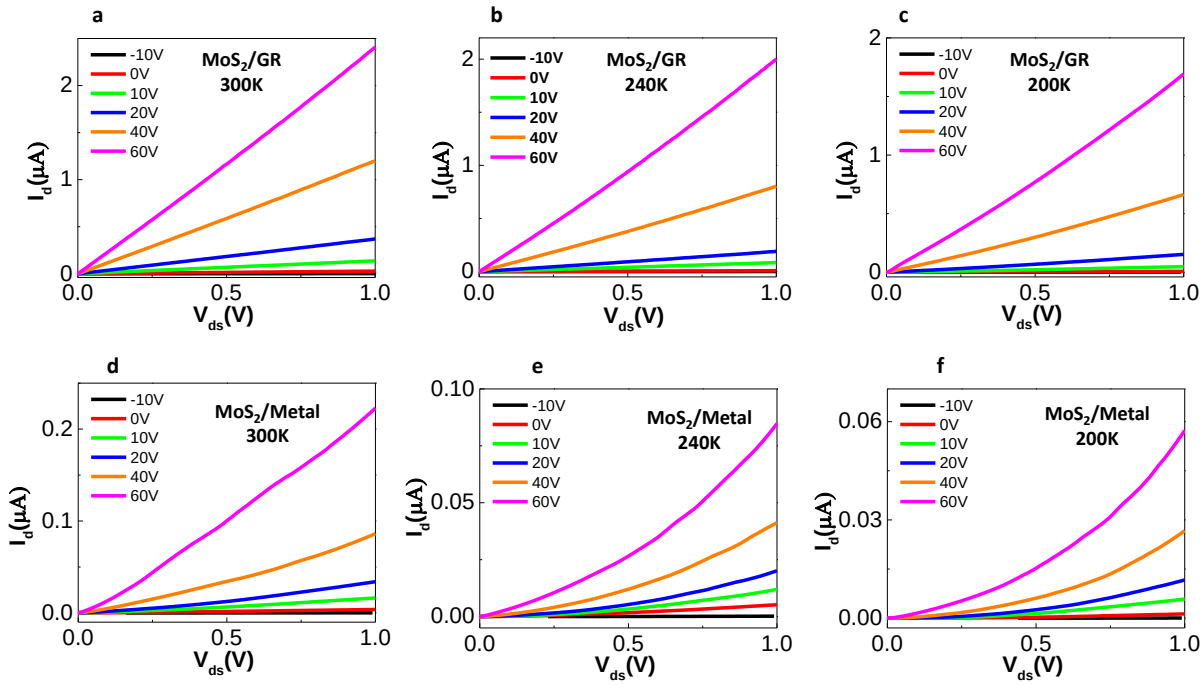

Figure S4. (a-f) I_d-V_{ds} measurements under different applied gate voltages for MoS_2/Gr and MoS_2/Metal FETs at 300 K, 240 K, and 200 K respectively.

S5. Electrical transfer characteristic for MoS_2/Gr and MoS_2/Metal FETs

The I_d-V_g measurements at different temperatures illustrate smaller temperature dependence for MoS_2/Gr than MoS_2/Metal transistor.

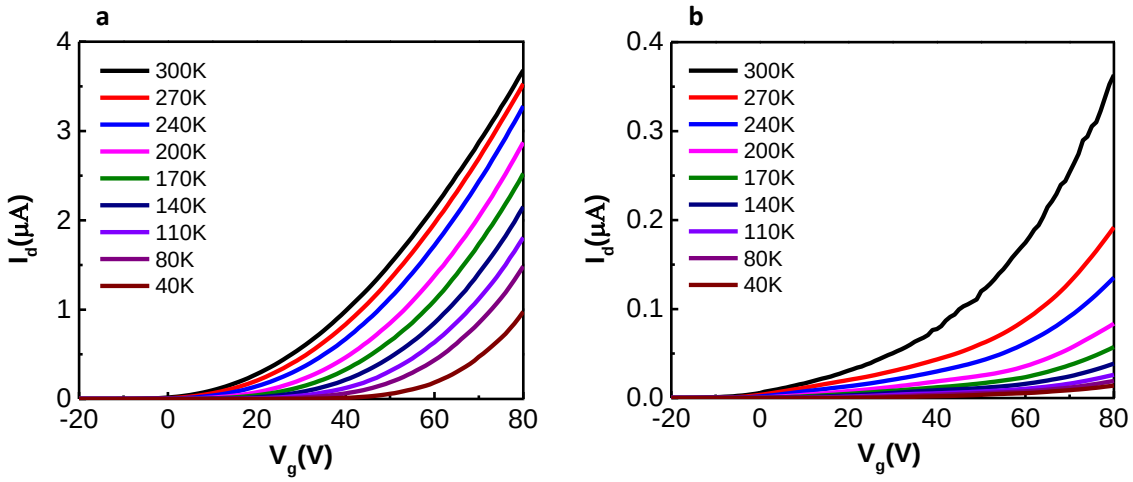

Figure S5. I_d-V_g measurements at different temperatures for **(a)** MoS_2/Gr and **(b)** MoS_2/Metal FETs.

S6. Extrinsic Field effect mobility of the MoS_2/Gr and MoS_2/Metal FETs

The Mobility calculation is based on the formula of $\mu = \left(\frac{dI}{dV_g}\right) \times \left(\frac{L}{WC_{ox}V_d}\right)$, where L/W is the ratio of the channel length/width, C_{ox} is capacitance between the channel and the back gate, I_d, V_d and V_g are drain current, drain-source voltage, and back gate voltage, respectively[2].

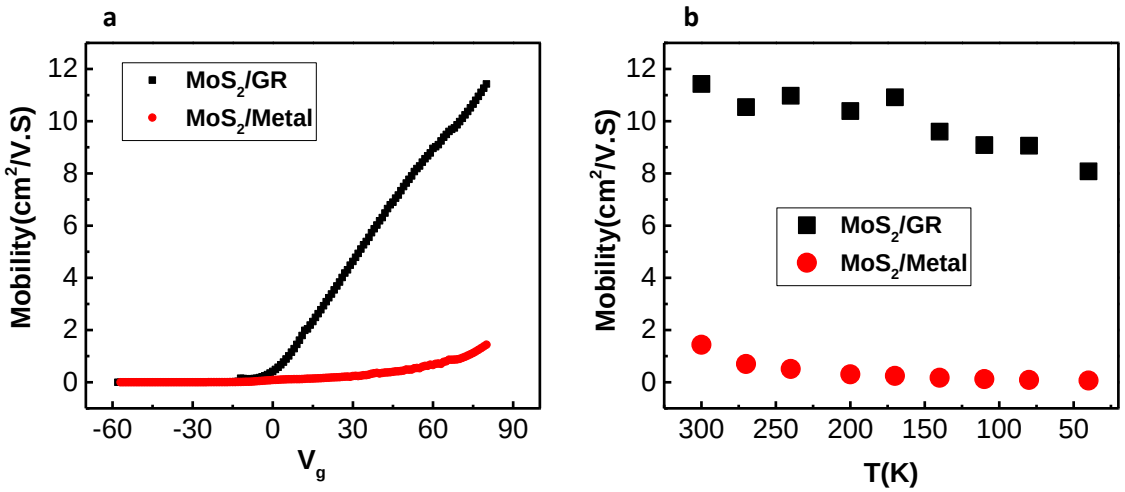

Figure S6. Mobility vs. **(a)** gate voltage at T = 300 K, and **(b)** the temperature at V_g = 80 V.

S7. Arrhenius measurements at constant V_g for different applied V_{ds}

Figure S7a and b show Arrhenius measurements of the MoS_2/Gr and MoS_2/Metal transistors at V_g=40 V for different applied source-drain biases respectively. To study the Schottky barrier height of the devices, a 2D thermionic equation $I_d=AT^{3/2}\exp\left(\frac{-q(\Phi_B-\frac{V_{ds}}{n})}{K_BT}\right)$ is used in which I_d is source-drain current, T is temperature, q is electron charge, K_B is Boltzmann constant, Φ_B is Schottky barrier height, V_{ds} is Source-drain current, n is Schottky diode non-ideality factor, and A is Richardson's constant[3,4].

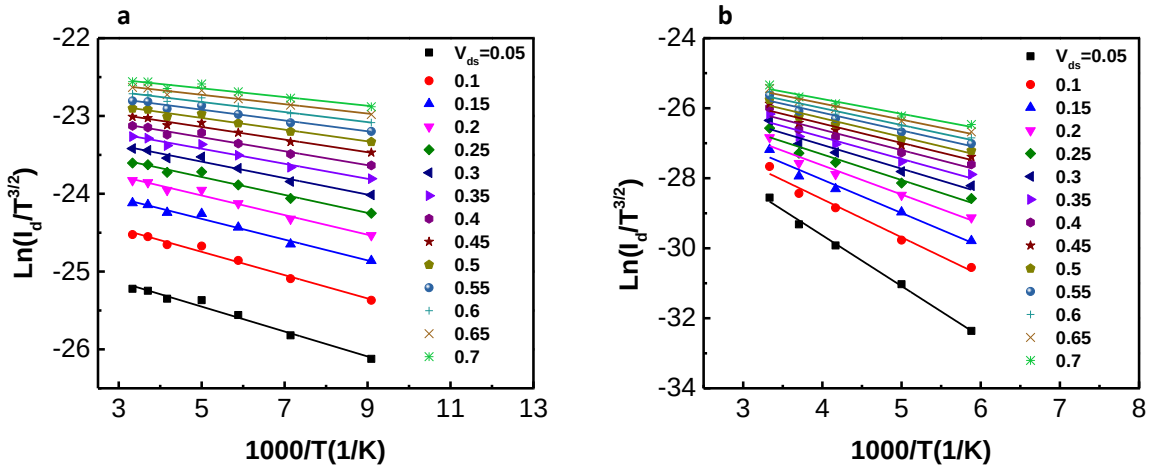

Figure S7. Arrhenius measurements for **(a),** MoS_2/Gr **(b),** MoS_2/Metal transistors at V_g=40V for different applied V_{ds}.

S8. Extracted Slope of the Arrhenius graph vs. the V_{ds} for MoS_2/Gr transistor

The slope of figure S7a ($\frac{-q(\Phi_B-\frac{V_{ds}}{n})}{K_BT}$) at each source-drain bias for V_g=40 V is derived and plotted in Fig S8 for the MoS_2/Gr in-plane heterostructure. Finally, the Schottky barrier height (Φ_B) is calculated at the intercept of Fig. S8 with the Y axis, where the V_{ds} is zero[3].

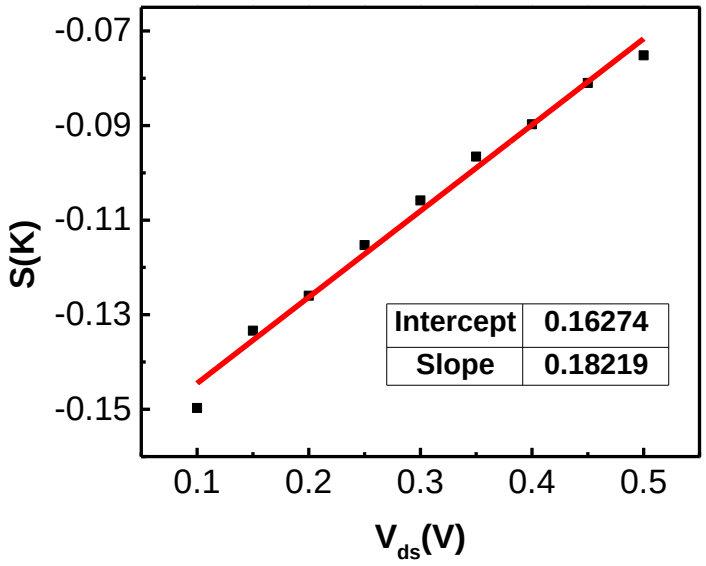

Figure S8. Slope of the Arrhenius graph as a function of the V_{ds} at gate 40 V.

S9. Arrhenius measurements at constant V_{sd} for different applied V_g

Arrhenius graphs are also plotted at constant V_{sd} for different applied gate voltages at room temperature as shown in Figure S9. Changing the slope of the Figure S9a from minus value at V_g=50 V to about zero at V_g=60 V and positive value at V_g=70 V also confirms the absence of the Schottky barrier for the MoS_2/Gr in-plane contact at gate biases close to the 60 V and above.

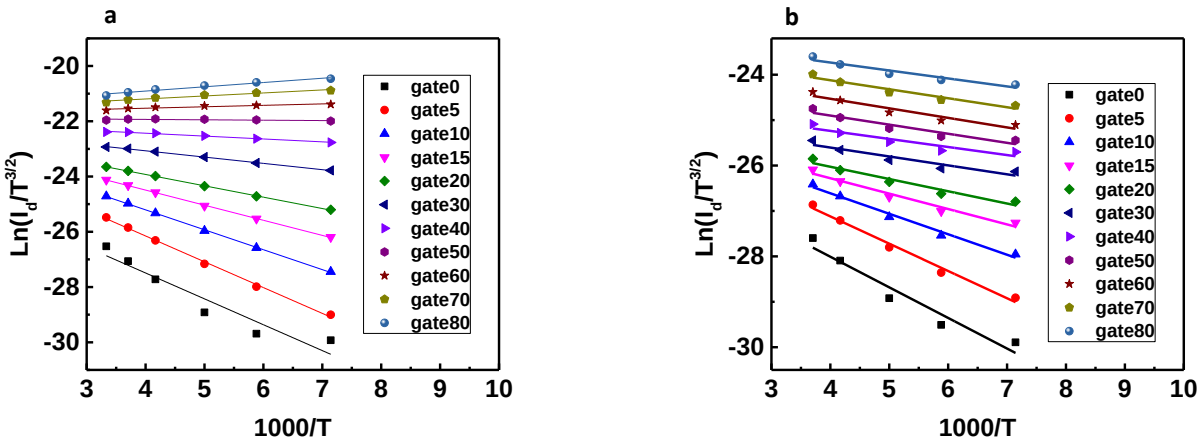

Figure S9. Arrhenius measurements for **(a)** MoS_2/Gr **(b)** MoS_2/Metal transistors at V_{sd} = 1V for different applied V_g.

S10. Kelvin probe force microscopy (KPFM)

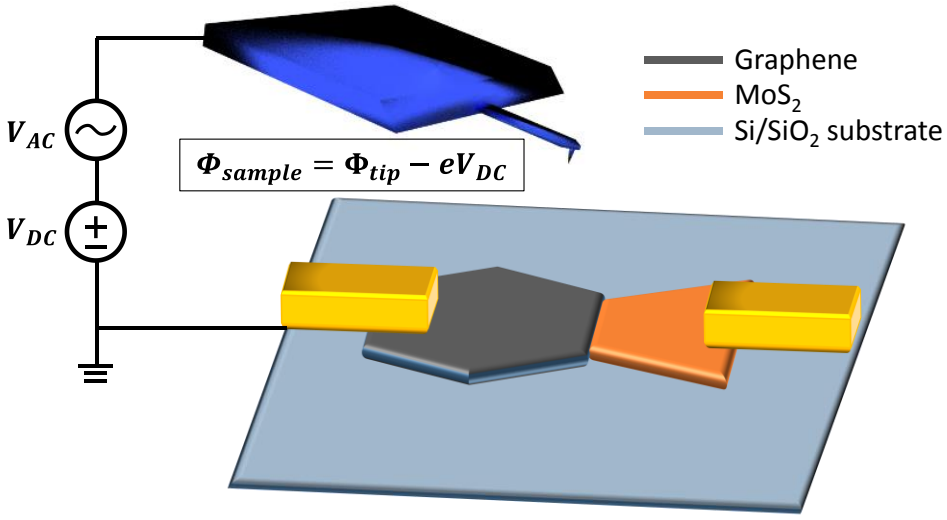

Figure S10. Schematic of the KPFM setup.

S11. 1/f Noise MoS_2-graphene

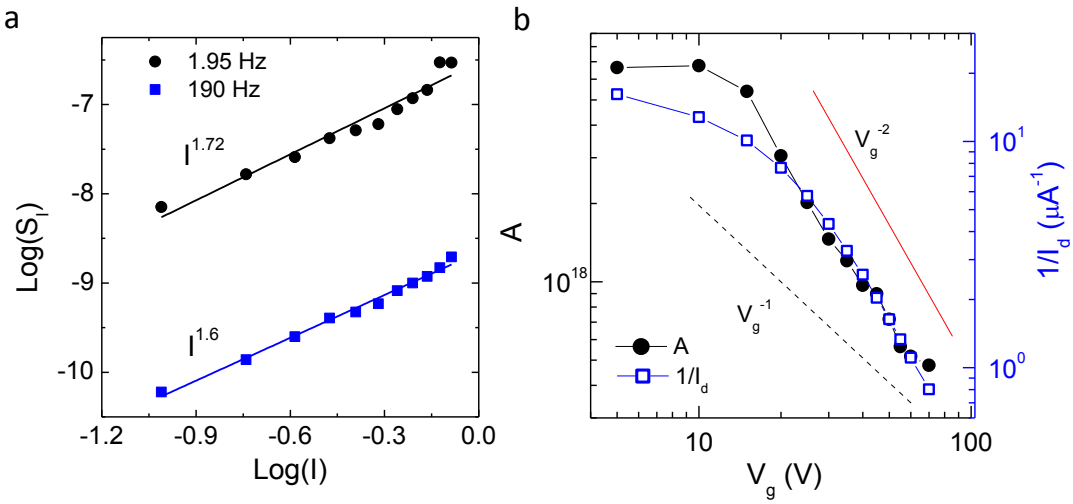

Figure S11. (a) Log(S_I) versus Log(I) of a MoS_2-graphene device showing $S \sim I^{\gamma}$ behavior with $\gamma = 1.72$ and 1.65 at 1.95 Hz and 190 Hz. V_g was kept constant at 40 V, and V_d was varied from 0.4 V to 4.4 V. (b) Noise amplitude A and $1/I_d$ is plotted as a function of V_g for $V_g > 0$. Dashed black line shows V_g^{-1} dependence and solid red line shows V_g^{-2}.

S12. 1/f Noise MoS_2-metal

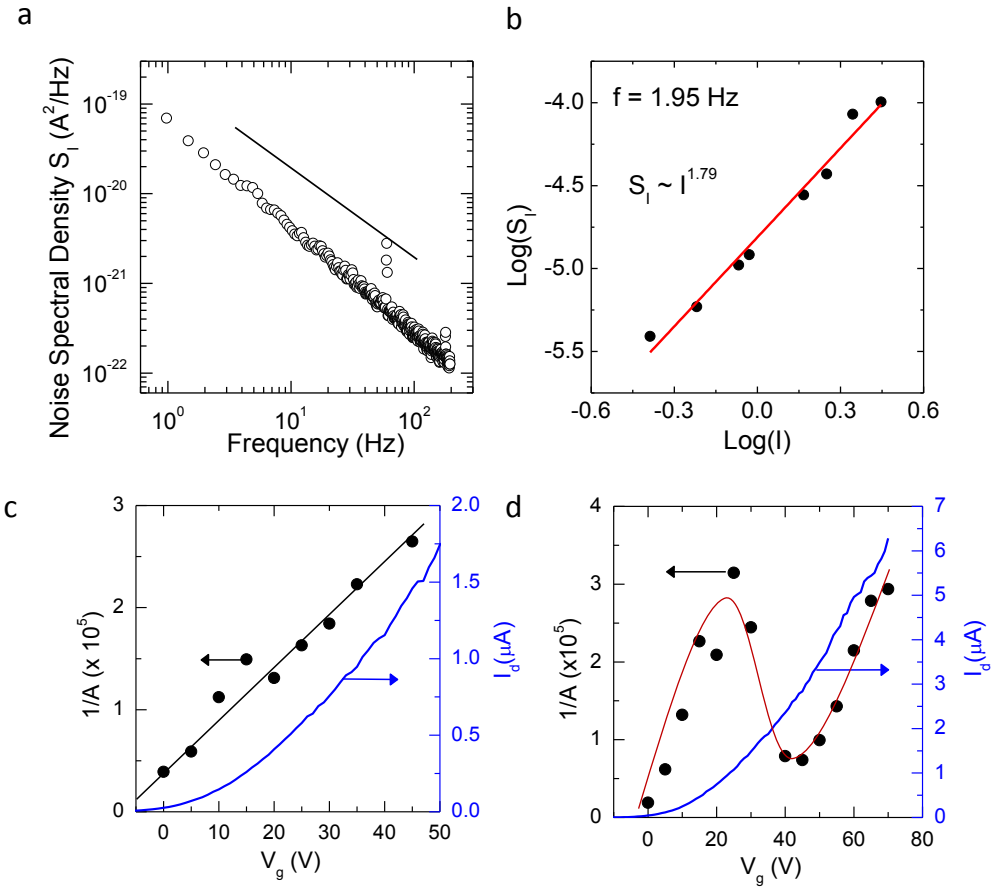

Figure S12. (a) Noise spectral density (S_I) versus frequency for a MoS_2-metal device at V_d = 2 V and V_g = 0 V showing $1/f^{\beta}$ with $\beta = 1.17$. The black line shows $\beta = 1$. **(b)** S_I versus I^{γ} behavior is established with $\gamma = 1.79$ at f = 1.95 Hz. **(c)** Inverse of noise amplitude (1/A) and I_d versus V_g for MoS_2-metal FET at V_d = 2 V. Black line is least square fit. **(d)** 1/A and device current (I_d) plotted as a function of gate bias V_g at V_d = 2 V. The red line is guide to the eye. The dip in 1/A at intermediate V_g values has been modeled in MoS_2 previously[5].

S13. Electronic band structure alignment between MoS_2 and graphene

At first, the band structures for graphene and MoS_2 are calculated separately from first principles using Density-Functional Theory. Then the bands are aligned at the interface using a semi-classical macroscopic model, often called Schottky-Mott rule, where their vacuum levels are matched at the interface and bands are aligned using their respective electron affinities and work functions. Schottky-Mott rule has been shown to reproduce band alignment quite well for 2D heterojunctions.[6–8]

The electron affinities of MoS_2 (χ_{MoS2}) and graphene (χ_{grap}) used in our calculation are 4.2 eV[9] and 4.55 eV[10]respectively; since the work functions depend on the position of the Fermi level, and hence also on the gate voltage, they are given by: $\phi = \chi + (E_c - E_F)$, where E_c represents the bottom of the conduction band and E_F is the fermi energy level. Since graphene is metallic, the barrier height ϕ_B, when seen from graphene towards the MoS_2, can be calculated by aligning their vacuum levels as: $\phi_B(V_g) = \phi_{grap}(V_g) - \chi_{MoS2}$. The amount of band-bending in MoS_2 at the interface is given by the difference in energies of the conduction band bottom at and away from the interface i.e. $\phi_{interface}(V_g) = \phi_{MoS2}(V_g) - \chi_{MoS2} - \phi_B(V_g)$.

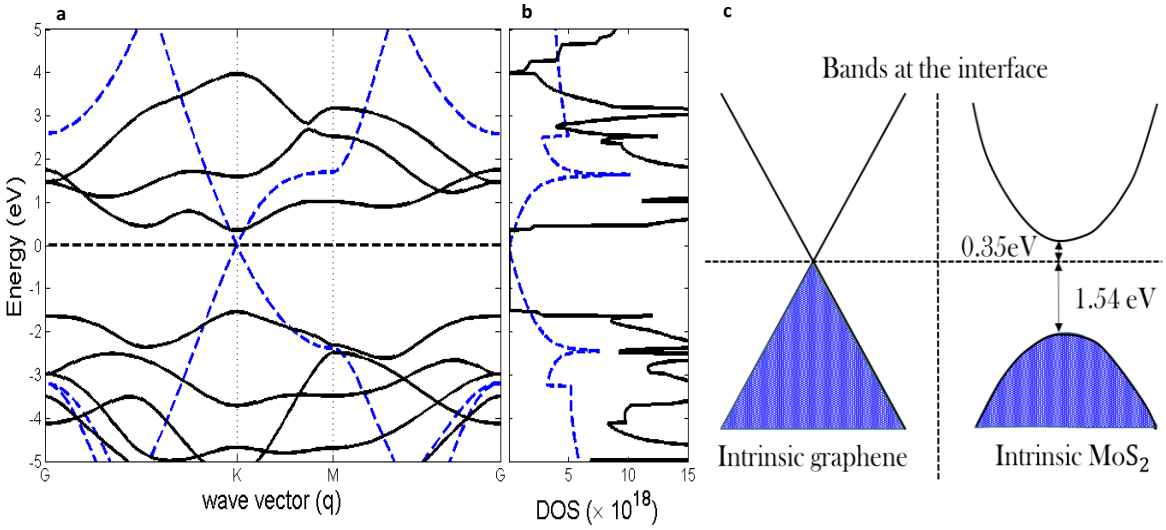

Figure S13: (a) Electronic band structure and **(b)** DOS of MoS_2 (solid black lines) and graphene (dashed blue lines) calculated from DFT using Quantum Espresso, showing the band alignment at the interface. There is a ϕ_B=0.35 eV barrier height at the interface **(c)** in the intrinsic case.

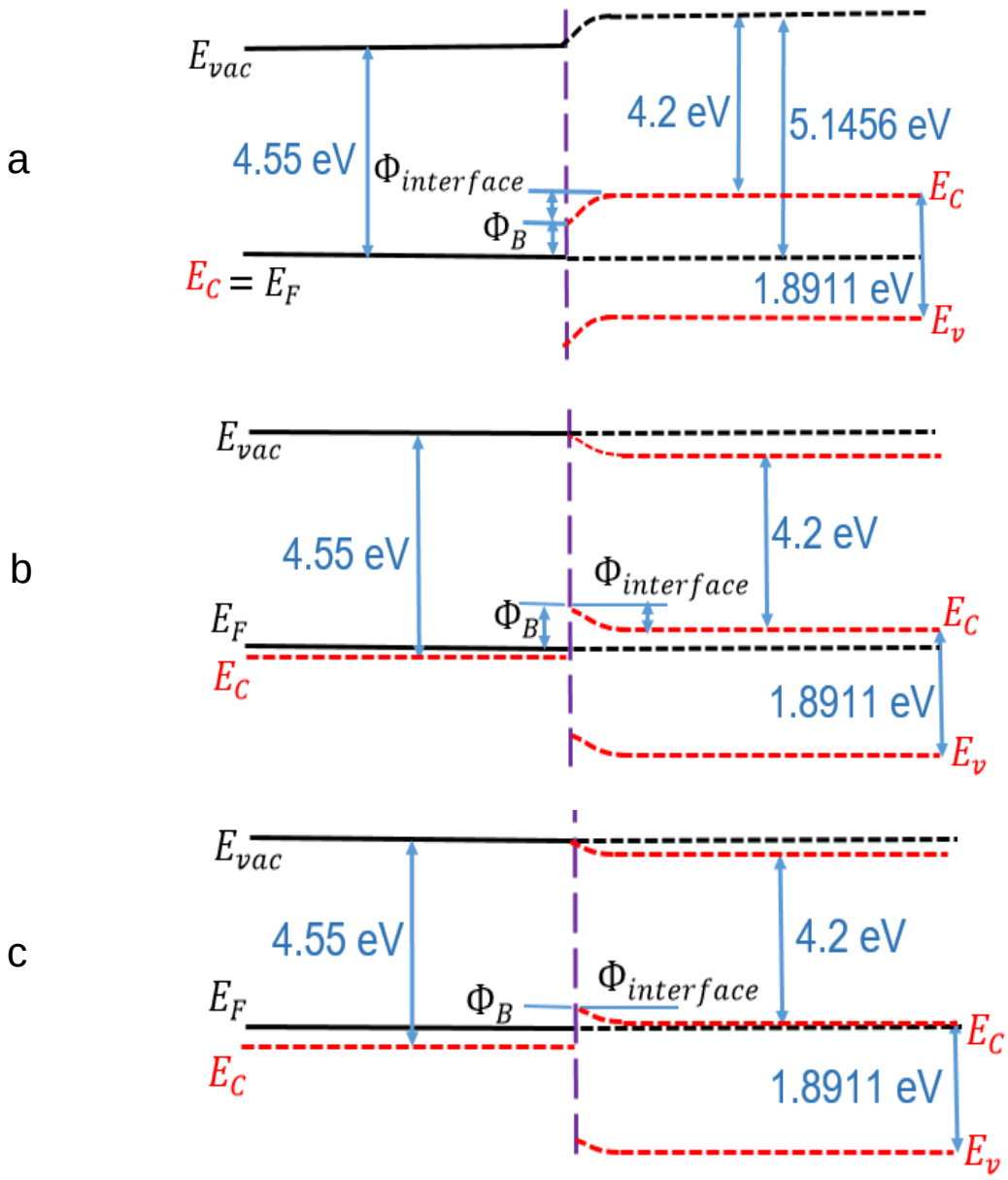

Figure S14. Band alignment between MoS_2 and graphene, showing the barrier height at the interface and band bending in the MoS_2, indicating an n-type Ohmic contact for **(a)** intrinsic graphene and MoS_2. There is a small barrier height for **(b)** extrinsic graphene and MoS_2 at V_g =0 V **(c)** at V_g =60 V. E_C in graphene on the left indicates the energy level of the Dirac point.

These calculations further reveal that even if there is a small overlapped region (a few nanometers) at the interface of graphene and MoS_2, the region of MoS_2 overlapping graphene is likely to be nearly-intrinsic, as dictated by band alignment at the interface. The MoS_2 in our

experiments is grown second, so the overlap region would have graphene in contact with the oxide and covered by a narrow region of MoS_2 on top of it. In the overlap region, the two materials are in contact and form an extended interface where the interface band alignment we describe above persists throughout the overlapping region. Consequently, the barrier between the gated graphene on the bottom and the MoS_2 on top of it remains significant. The carrier concentration in the MoS_2 remains relatively small, qualitatively similar to the conditions observed at $V_G = 0$, as the graphene effectively screens the electric field from reaching the MoS_2 layer. The electrons traveling from graphene to the MoS_2 on top of it in the overlapping region then experience a very large series resistance from the nearly intrinsic MoS_2 region on top of graphene, before they reach the non-overlapping gated portion of MoS_2. Based on the band alignment at the interface, we calculate the conductivity of the MoS_2 region on top of graphene using the mobility calculation described in Experimental Section. We find the resistance of the top MoS_2 region to be dependent on the specific V_G as the gate voltage also impacts the band alignment at the interface and thus also influences the carrier concentration in the overlapping MoS_2 region. Under all gate voltages we investigated, the carrier concentration of MoS_2 in the overlap was found to be much smaller than graphene or the non-overlapping portion of the MoS_2, consistent with previous studies for gated vertical stacks which found that MoS_2 transfers most of its electrons into the graphene below it,[11] where the authors found that the metallic graphene screens out the electric field from penetrating to the MoS_2, thereby making the gating of the top layer inefficient and causing $R_{MoS2} >> R_G$. Similarly, we found the overlapping region of MoS_2 to be highly resistive, as calculated based on the procedure we described in Experimental Section. The total resistance is dependent on the width W and length L of the overlap, but for our device dimensions and assuming 10 nm overlap we find it to be more than

two orders of magnitude higher than the contribution of the interface R_{int}, described in the manuscript. Our calculations are summarized in the following table:

V_G	Φ_B	R_G	R_{MoS_2}	$R_{int.}$	$R_{overlap}$ (10 nm L)
V	eV	ohm	ohm	ohm	ohm
0	0.2943	4e3	3.2e7	6.3e6	8e8
10	0.2369	1.4e3	6.9e6	6.1e5	1e8
20	0.1959	897	2.8e6	1.3e5	2.2e7
30	0.1619	660	1.5e6	-	5.1e6
40	0.1322	534	9.18e5	1.1e4	1.5e6
50	0.1055	457	6.13e5	-	6.3e5
60	0.0813	404	4.3e5	1.5e3	1.7e5
70	0.0588	367	3.2e5	-	5.5e4
80	0.0379	340	2.5e5	-	1.5e4

Because of the large added resistance $R_{overlap}$ of the top MoS_2 layer, it is much less likely the current would flow vertically from graphene to the highly resistive MoS_2 on top. The less resistive current path will be through the highly conductive graphene below the MoS_2 to the lateral graphene-MoS_2 interface, followed by transport through the lateral interface and into the gated (non-overlapping) portion of the MoS_2. Hence, we expect our results to be relatively independent of overlapping, as long as the MoS_2 is on top of the graphene. Note that the situation would be reversed if graphene were on top; the less resistive path would again be through graphene. The resistance of the graphene would be smaller than that of the MoS_2 below it owing to the large contrast in carrier mobility of the two materials. The least-resistance current path would again be through the graphene on top of MoS_2 and then through the graphene-MoS_2 interface and the total resistance would depend on the width of the overlapping region. This is

not the situation in our work because MoS_2 is grown second so it is always on top of graphene in the narrow region where they overlap.

References:

[1] X. Ling, Y. Lin, Q. Ma, Z. Wang, Y. Song, L. Yu, S. Huang, W. Fang, X. Zhang, A. L. Hsu, Y. Bie, Y. H. Lee, Y. Zhu, L. Wu, J. Li, P. Jarillo-Herrero, M. Dresselhaus, T. Palacios, J. Kong, *Adv. Mater.* **2016**, *28*, 2322.

[2] A. Dankert, L. Langouche, M. V. Kamalakar, S. P. Dash, *ACS Nano* **2014**, *8*, 476.

[3] J. R. Chen, P. M. Odenthal, A. G. Swartz, G. C. Floyd, H. Wen, K. Y. Luo, R. K. Kawakami, *Nano Lett.* **2013**, *13*, 3106.

[4] E. Kaxiras, J. Kong, H. Wang, *Nano Lett.* **2014**, *14*, 3055.

[5] X. Xie, D. Sarkar, W. Liu, J. Kang, O. Marinov, M. J. Deen, K. Banerjee, *ACS Nano* **2014**, *8*, 5633.

[6] Z. Lin, A. McCreary, N. Briggs, W. Zhang, Q. Wang, Y. Chen, A. Kumar, P. K. Ahluwalia, S. Zhu, Y. Ni, J. Liu, B. Ha Nguyen, V. Hieu Nguyen, B. Ram, A. Manjanath, A. K. Singh, J. Sophia Ponraj, Z.-Q. Xu, S. Chander Dhanabalan, Z.-K. Tang, C.-J. Tong, W. Geng, X. Qian, Y. Wang, W. Li, C. Zhang, C. Gong, Y. Nie, K.-A. Min, C. Liang, Y. Jun Oh, H. Zhang, W. Wang, S. Hong, L. Colombo, R. M. Wallace, K. Cho, *2D Mater* **2017**, *4*, DOI 10.1088/2053-1583/4/1/015026.

[7] J. Zhang, W. Xie, J. Zhao, S. Zhang, *2D Mater.* **2016**, *4*, 15038.

[8] H. Yu, A. Kutana, B. I. Yakobson, *Nano Lett.* **2016**, *16*, 5032.

[9] M. S. Choi, G.-H. Lee, Y.-J. Yu, D.-Y. Lee, S. H. Lee, P. Kim, J. Hone, W. J. Yoo, *Nat. Commun.* **2013**, *4*, 1624.

[10] J.-T. Seo, J. Bong, J. Cha, T. Lim, J. Son, S. H. Park, J. Hwang, S. Hong, S. Ju, *J. Appl. Phys.* **2014**, *116*, 84312.

[11] C. Shih, Q. H. Wang, Y. Son, Z. Jin, D. Blankschtein, M. S. Strano, *ACS Nano* **2014**, *8*, 5790.